

Efficient Synthesis for a Wide Variety of Patellamide Derivatives and Phosphatase Activity of Copper-Patellamide Complexes

Philipp Baur,^[a] Peter Comba,^{*[a]} and Gunasekaran Velmurugan^[a]

Abstract: Copper complexes of patellamides have shown catalytic activity in a variety of reactions but their biological function remains unknown. There are significant differences between the natural macrocycles and synthetic analogues in the various catalytic activities. It therefore is essential to be able to perform in vivo and ex vivo reference measurements with the natural patellamide macrocycles, very similar derivatives and a large range of synthetic analogues. The preparative method described allows for a highly adaptable synthetic

process producing building blocks for a large range of patellamide derivatives: apart from natural compounds, a new synthetic patellamide was prepared that does not have any substituents at any of the four heterocycles. Together with the variation of substituents at the aliphatic backbone, this allowed to elucidate the catalytic activity for phosphoester hydrolysis as a function of the structure and dynamics of the dicopper(II)-patellamide complexes, both by experiment and DFT-based mechanistic studies.

Introduction

Patellamides have attracted the interest of scientists from various disciplines since their discovery in the 1980s.^[1] Originally discovered by medical researchers in search of marine compounds for pharmaceutical applications, the formation of stable mono- and dinuclear copper(II) compounds and their catalytic proficiency have attracted the interest of scientists from various areas. The rigid macrocyclic backbone offers a high degree of preorganization for cooperative metal ion binding, especially with copper(II).^[2–4] The complexes have shown the ability to catalyze a wide range of reactions of potential metabolic relevance, such as carbonic anhydrase, phosphatase, β -lactamase and glucosidase. The true biological function of these interesting macrocycles and their metal complexes, however, is not yet known.^[5,6] A recent study has shown, that fluorescence-labeled patellamide analogues bind copper(II) ions in vivo,^[4] and this, together with the known complex stabilities (specifically Cu^{II} vs. Zn^{II}) and the observed accumulation of Cu^{II} in ascidians (approx. 10⁴-fold vs. the surrounding seawater), supports the general assumption that the copper(II) coordination chemistry of patellamides is of biological relevance.^[3,6,7]

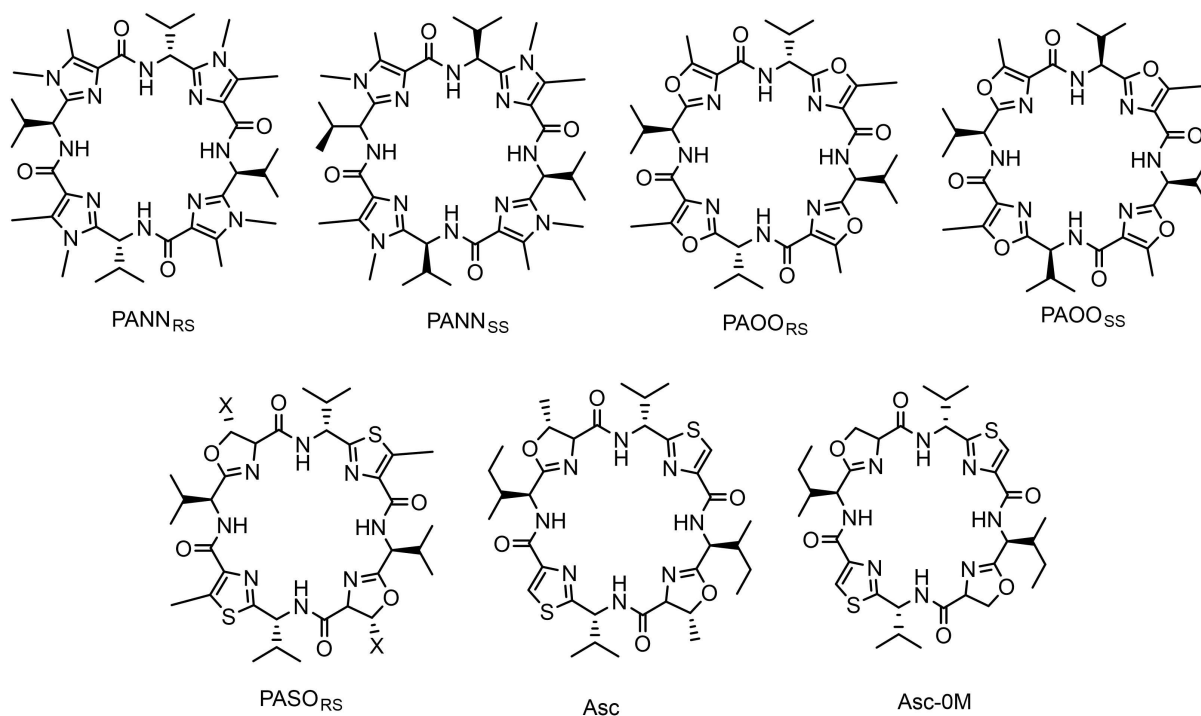
The class of peptides referred to as patellamides are cyclic octapeptides, in which four of the peptide bonds have enzymatically been heterocyclized to thiazole or oxazoline (derived from cysteine and serine or threonine, respectively; see Scheme 1 for structures of patellamide derivatives). So far, patellamide derivatives have only been found in ascidians of the species *Lissoclinum patella*, where they are produced in vast amounts of up to several percent of the organism's dry mass.^[8] Taxonomic studies have shown that, while the macrocycles are found all over the organism, they are produced by one of its cyanobacterial symbionts, *Prochloron didemni*, which has the genes required for the patellamide biosynthesis.^[8] This cyanobacterium is an obligate symbiont and has so far not been found alone or in symbiosis with any other organism. Since all attempts to cultivate *P. didemni* have failed so far, it is likely that the symbiosis with the ascidians plays a crucial role for the survival of the cyanobacterium.^[9] The basis of the symbiotic relationship might be the exchange of nutrients, with the cyanobacterium supplying its host with photosynthesis products and the ascidians providing nitrogen-based waste products for the cyanobacteria to recycle. Amongst the molecules exchanged, patellamide derivatives are one of the largest groups, suggesting a pivotal role for the organisms. Since previous studies have shown the ability of copper(II) patellamide complexes to catalyze a wide range of reactions, it is possible that the patellamide copper(II) compounds' function is of an enzymatic nature. However, due to the demanding preparative procedures, most evaluations of the catalytic activity of copper(II) patellamide complexes have used synthetic patellamides with imidazole donors and simplified side chains at the macrocycle backbone.

The most efficient catalysis with copper(II) patellamide complexes reported so far is carbonic anhydrase activity: it was shown that the dicopper(II) complexes with natural and artificial patellamides catalyze the hydrolysis of CO₂ only approx. 2

[a] P. Baur, Prof. Dr. P. Comba, Dr. G. Velmurugan
Universität Heidelberg
Anorganisch-Chemisches Institut und
Interdisziplinäres Zentrum für Wissenschaftliches Rechnen
Im Neuenheimer Feld 270, 69120 Heidelberg (Germany)
E-mail: peter.comba@aci.uni-heidelberg.de

Supporting information for this article is available on the WWW under <https://doi.org/10.1002/chem.202200249>

© 2022 The Authors. Chemistry - A European Journal published by Wiley-VCH GmbH. This is an open access article under the terms of the Creative Commons Attribution Non-Commercial NoDerivs License, which permits use and distribution in any medium, provided the original work is properly cited, the use is non-commercial and no modifications or adaptations are made.



Scheme 1. The patellamide analogues (PA) used for experimental and theoretical studies in this paper and ascidiacyclamide (Asc), one of the most common patellamide derivatives in nature. Ascidiacyclamide-0 M (Asc-OM) is not known to occur in nature but is structurally very similar to patellamide A and ascidiacyclamide.

orders of magnitude more slowly than enzymes but faster than any known small molecule model system. Interestingly, the enzymes as well as most of the model systems are generally mononuclear zinc(II) species, and the copper(II)-patellamide complexes would indeed be the only known dinuclear copper(II) carbonic anhydrases, if this would be their biological function.^[2,10] Importantly, the carbonic anhydrase activity was shown to be strongly dependent on the type and stereochemistry of the side chains at the macrocycle backbone and to a much lesser extent from the heterocycles. For other catalytic reactions, such as the phosphatase discussed in the present communication, it appears that the naturally occurring heterocycles thiazole and oxazoline lead to enhanced activity, and this could be due to subtle electronic effects and/or the flexibility due to the loss of aromaticity in oxazoline (see below). The side chains at the patellamide scaffold and in particular their stereochemistry on the other hand seem to influence the shape and stiffness of the backbone, and they may therefore also provide a type of channel that facilitates substrates to reach the catalytic site.^[3,10,11]

To obtain the patellamides from biological sources in order to study properties of the natural patellamides is not appropriate for ecological and economic reasons. It therefore was deemed necessary to obtain the natural products and very similar derivatives synthetically. The biosynthetic approach has been considered but due to only small amounts obtained in the biosynthesis at often great efforts to isolate pure samples,^[8] the total synthetic approach seemed to have advantages. Shortly after the discovery of the patellamides, various synthetic

approaches were developed but these methods generally were tedious and often did not allow to prepare a wide range of derivatives and significant amounts of the macrocycles.^[12–15] There are two main strategies based on modern peptide synthesis for the synthesis of Patellamide A and several patellamide analogues.^[16,17] While the total synthetic approach for Patellamide A allows preparing the natural product,^[16] the heterocyclizations of peptide side chains using Burgess-Reagent^[17] are an elegant method for the synthesis of a wide range of natural and artificial patellamide derivatives but the preparation of specific macrocycles – including some of the natural products – can be tedious and sometimes little reliable.^[2,3,18] The approach used up to now involves the synthesis of building blocks that are coupled to obtain the desired macrocycle but the heterocyclization methods previously used are not appropriate for the naturally occurring non-methylated thiazole rings.^[17] Moreover, the available synthetic schemes cannot easily be adapted to modern solid phase (SPPS) methods if they require prolonged refluxing or stirring.

Here, we report a new, efficient and general approach for the synthesis of naturally occurring patellamides and a wide range of artificial derivatives, which were not available before. The approach is based on the optimized synthesis of a large variety of stable pseudo-dipeptide and pseudo-tetrapeptide building blocks that may be coupled in any combination to yield patellamide-type macrocycles with a virtually unlimited range of heterocycle, macrocycle sidechain and stereochemistry patterns, including the natural products as well as model substances that were not accessible so far. The corresponding

dicopper(II) complexes were prepared and used for phosphatase studies as an example of a possible enzymatic model reaction. Phosphatase was chosen as the model reaction because it is experimentally less demanding than the possibly more relevant carbonic anhydrase reaction, and also because the basic mechanism is very similar. Moreover, a large range of published data with patellamide macrocycles as well as with other ligand systems and with a range of different metal ions is available. The catalytic efficiency was probed in dependence of steric and electronic variations of the macrocycle structure, and the influence of the stereochemistry and steric bulk of the side chains was interpreted based on a preliminary DFT-based quantum-chemical analysis.

Results and Discussion

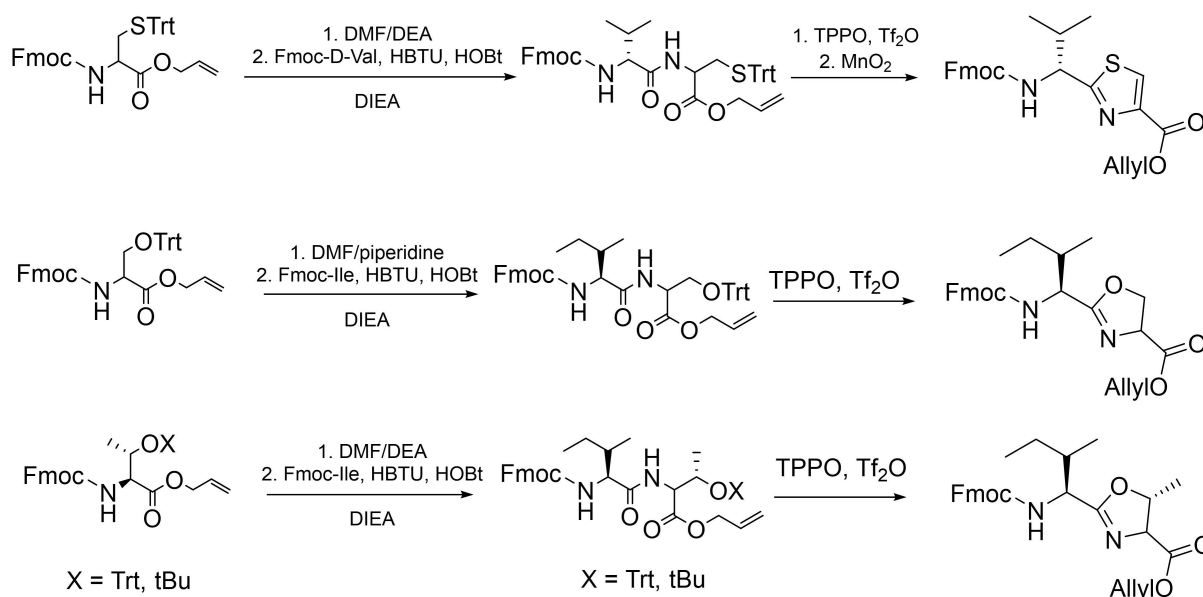
Patellamide synthesis

In order to take profit from the previous methods, new building blocks were developed that can flexibly be chosen to lead to any desired macrocycle including the natural products. The peptides were N-protected with Fmoc, and allyl alcohols were used to protect the carboxylate; sulfur in cysteine and hydroxide were protected using triphenylmethane (Trt) or tert-butyl (t-Bu) protecting groups. All protecting groups were chosen due to their availability and compatibility with the synthetic conditions. The heterocyclizations of the dimeric building blocks were performed using triphenylphosphine oxide (TPPO) and trifluoromethanesulfonic anhydride (Tf₂O) for both thiazole and oxazoline building blocks.^[19–24] Since the heterocyclization of cysteine leads to dihydrothiazoles instead

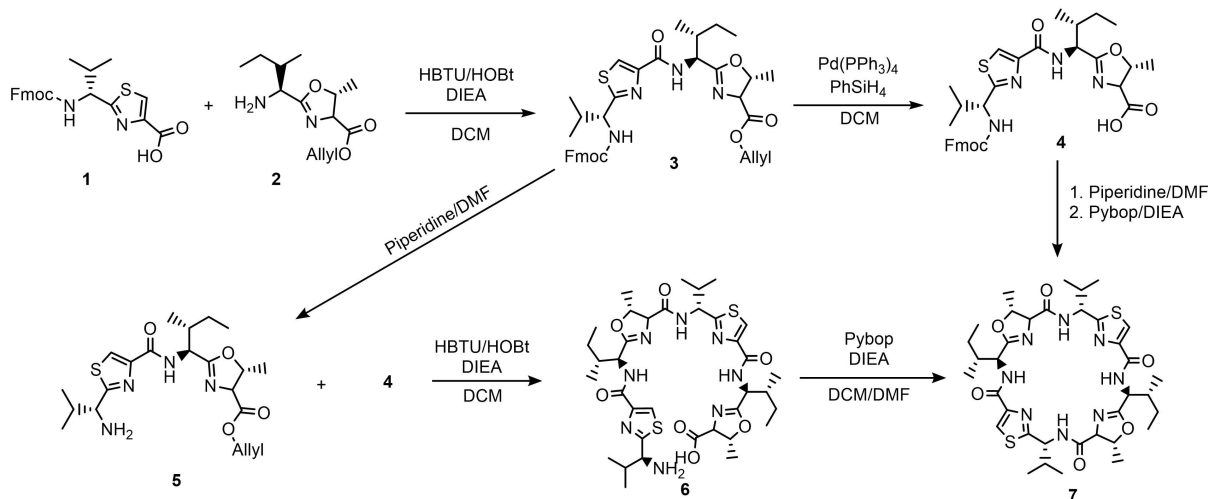
of thiazoles, an oxidation step using nanoparticulate activated MnO₂ follows the heterocyclization (see Scheme 2).^[25,26]

Since the heterocyclization step to oxazoline occurs at an early stage of the synthesis, our approach allows for a straightforward, adaptable and scalable synthesis of a large range of patellamide-derived macrocycles and also allows for side-by-side preparation of the building blocks. This permits to obtain natural patellamides as well as artificial derivatives at larger scales for biomimetic studies, catalysis and pharmaceutical applications. The building block approach is also relevant for possible solid phase syntheses. The heterocyclic building blocks described here can be produced in comparably large amounts using liquid phase chemistry and can be stored for prolonged periods of time. Peptide coupling was done using the well-established HOBt/HBTU/DIEA based coupling procedures (see Scheme 2).

Generally, there are two possible approaches to obtain the final patellamides from the building blocks. These are singly deprotected (one on the acid, one on the amine side) and coupled to a dimeric building block, then the dimeric building block can be deprotected on both sides and directly cyclodimerized to the desired patellamide.^[17] For this cyclodimerization, several possible reagents have been attempted (DPPA, FDPP, HATU), with FDPP having shown the best results (see Scheme 3). Alternatively, the dimer is split into two fractions, one to be deprotected on the amine side the other on the acid side. The resulting deprotected tetrapeptides are coupled to form the octapeptide. This is deprotected on both sides and macrocyclized by slowly injecting it into a solution of Pybop and DIEA.^[16] The imidazole- or oxazoline-based derivatives were synthesized using the synthetic approach described in the literature.^[17]



Scheme 2. Description of the synthesis of the three main building blocks: formation of the dipeptide by coupling one amino acid with a hydrophobic side chain (Ile/Val) with another with a polar neutral side chain (Cys, Ser, Thr), followed by heterocyclization to the corresponding heterocyclic building block HC, HS or HT; in case of the thiazole building block HC, the coupling is followed by oxidation with activated MnO₂ to obtain the aromatic thiazole.^[25,26]



Scheme 3. Synthetic strategy from the various possible building blocks (see Scheme 2; 1 and 2 are examples that can be substituted by any other building block) via the dimerized tetrapeptides towards the final macrocyclic octapeptides.

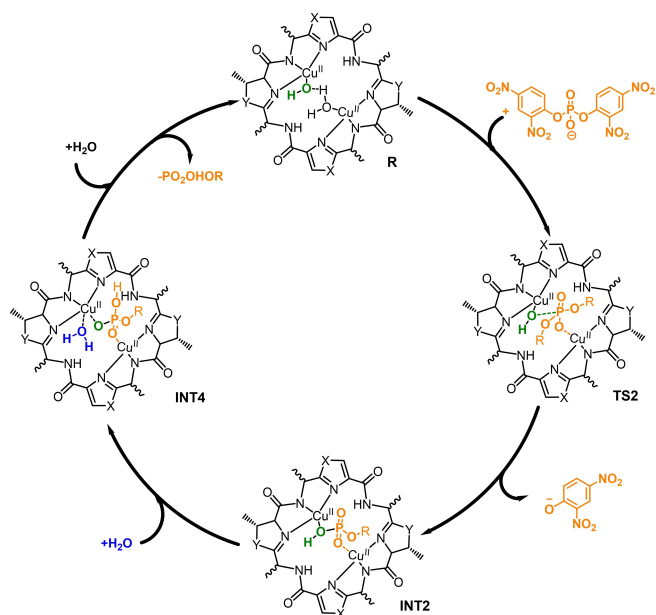
Apart from the naturally occurring derivatives such as ascidiacyclamide (see Scheme 1), the method described in Schemes 2 and 3 also allows for the synthesis of new derivatives, using for example serine instead of threonine as reactant for the oxazoline building block. The resulting macrocycle is very similar to the natural product but the bonding to copper(II), the structure of the dicopper(II) complex and, importantly, the interaction of the complex with substrates in catalytic transformations might be significantly different. These effects, which currently are studied both experimentally and computationally, and which are only possible to understand in detail when the synthetic methods are available to efficiently prepare the macrocycles and their complexes, will deepen our understanding of the principles behind the reactivity of the dicopper(II) patellamide type catalysts. Described in the next sections are therefore a preliminary computational analysis of phosphatase as one of the possible and possibly biologically relevant catalytic transformations of copper(II)-patellamide systems,^[3,4,27,28] together with the experimental evaluation of various patellamide derivatives in terms of their phosphatase efficiency.

Phosphodiesterase activity – DFT based predictions

Catalytic transformations of dicopper(II)-patellamide sites of putative biological relevance for the ascidians that have been studied include carbonic anhydrase,^[2,10] phosphatase,^[4,27,28] lactamase and glycosidase reactions.^[29] As indicated before, and as expected and observed, the catalytic efficiency strongly depends on the structure of the dicopper(II) complex, and this is largely enforced by the heterocyclic donor groups, the flexibility of the heterocycles, the stereochemistry of the side chains and their steric bulk.^[2–4] Apart from variations in their rigidity (oxazole and thiazole vs. their partially reduced and more flexible oxazoline and thiazoline derivatives), the basicity

of the various heterocycles is the major difference (pK_a , imidazole: 7.0,^[30] thiazole: 2.5,^[30] oxazoline: 4.75,^[31] oxazole: 0.8).^[30,32] Metal-ligand bonding largely depends on the basicity of the donor, and this is expected to influence the complex stability as well as the electron distribution in the complex and therefore also the acidity of the coordinated OH_2 , that is, the availability of OH^- as a nucleophile in catalytic hydrolysis reactions. However, from experimentally determined complex stabilities it appears that the various heterocycle combinations only have a minor effect on the stability constants,^[3] and the optimum pK_a values for the various catalytic hydrolyses, experimentally obtained from the typical bell-shaped curves (see Supporting Information), also do not appear to differ significantly with variation of the heterocycles. Therefore, the main differences related to the various heterocycle combinations are subtle structural changes (see below).

There are only few crystal structures of patellamide-copper(II) complexes available.^[18,33] However, solution structural information is more relevant than solid-state geometries to understand the catalytic activities, and the combination of EPR spectroscopy with structural modeling has allowed to obtain accurate structural data of dipole-dipole-coupled dicopper(II) systems in general,^[34–36] and specifically also of copper(II)-patellamide complexes.^[2,37] The mechanisms of catalytic transformations, in particular for phosphatase and carbonic anhydrase have been studied in some detail experimentally,^[2,10, 27, 28] and for the carbonic anhydrase also by a thorough DFT analysis.^[38] The mechanism of the phosphoester hydrolysis derived from these studies is shown in Scheme 4. In order to be able to predict and interpret the reactivity as a function of the macrocycle used, the energy barrier of the putative rate determining step, describing the attack of the $\text{Cu}^{\text{II}}\text{-OH}$ nucleophile at the phosphorous center (TS2) to yield a phosphate (or phosphoester) bridged dicopper(II) intermediate (INT2) was studied in a preliminary DFT analysis (in order to limit the computational expense a dimethyl ester of phosphate



Scheme 4. Proposed catalytic cycle for the dicopper(II)-patellamide catalyzed phosphoester hydrolysis. Additional water molecules bound to the copper(II) centers are omitted for clarity. The full reaction cycle used for the calculations is given as Supporting Information (Scheme S1).

was used as substrate instead of the experimentally used bis-dinitrophenylphosphate).

The results suggest significant differences between different previously studied patellamide derivatives with 1,5-dimethylimidazoline heterocycles (PANN_{SS}, PANN_{RS}) and thiazole-oxazoline-based derivatives (Asc, Asc-OM). Macrocycles with structures similar to the naturally occurring Patellamide A, Patellamide C and Ascidiacyclamide with various side chain conformations and heterocyclic donor groups show interesting differences in the calculated barrier of the rate determining step (attack of the OH⁻ nucleophile at the phosphorous center, TS2). The computed barriers suggest that the type of heterocycle, as well as the nature and stereochemistry of the side chain, have an influence on the catalytic efficiency (see Figure 1).

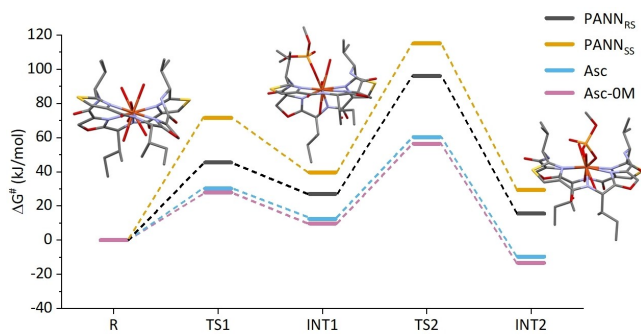


Figure 1. DFT/B3LYP-D3 (PCM; MeOH) computed free energy profile (kJ/mol) of the phosphatase reaction according to Scheme 4, catalyzed by PANN_{RS}, PANN_{SS}, Asc and Asc-OM.

The substrate bis-dinitrophenylphosphate (BDNPP), generally used in experimental studies, has been substituted in the calculations by the computationally less demanding dimethyl ester. The energy scheme in Figure 1 shows the results of the preliminary DFT analysis. In the first step of the catalytic sequence, the substrate binds to one of the Cu^{II} centers and substitutes an OH₂ to yield structure INT1 with an energy barrier between 71.6 kJ/mol (PANN_{SS}) and 27.9 kJ/mol (Asc-OM; see Supporting Information for details). The attack of the hydroxy group coordinated to the second Cu^{II} center at the bound phosphoester in the rate determining step requires barriers between 115.1 kJ/mol (PANN_{SS}) and 56.4 kJ/mol (Asc-OM). Plots of the refined structures of the rate determining transition state involving the attack of the nucleophile are given in Figure 2.

The most interesting observation from the energy scheme in Figure 1 is that the stereochemistry of the side chains has a substantial influence on the barrier of the rate-determining step (PANN_{SS} vs. PANN_{RS}: 115.1 kJ/mol, 96.0 kJ/mol) but the difference is significantly smaller than that due to the type of heterocycle (PANN_{RS} vs. Asc: 96.0 kJ/mol, 60.3 kJ/mol, Asc-OM: 56.4 kJ/mol). Importantly, this is also what is observed experimentally, that is, the catalytic rates depend on both, the configuration and the heterocyclic donor, and the increase in efficiency with the natural heterocycles instead of imidazole derivatives is more important than the macrocycle side chains and their configurations (see below). The situation is entirely different for the dicopper(II)-patellamide catalyzed carbonic anhydrase, where experimental data indicate that the two catalysts with PANN_{RS} and Asc, with identical – that is, naturally occurring – stereochemistry of the side chains, both are much more efficient catalysts than all other studied dicopper(II)-patellamide carbonic anhydrase catalysts with different heterocyclic donors but all with the unnatural S,S,S,S configuration at the macrocycle side chains (e.g. PANN_{SS} vs. PANN_{RS}),^[10] and this experimental observation is supported by a DFT analysis.^[38]

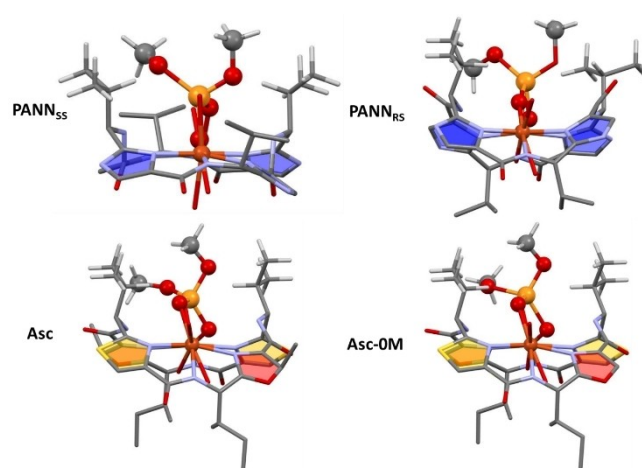


Figure 2. Optimized geometries of TS2 of the phosphatase reaction catalyzed by PANN_{RS}, PANN_{SS}, Asc and Asc-OM (only selected hydrogen atoms are shown for clarity; the heterocycles are colored with the usual color code; the view is through the two copper(II) centers, and the center with the attacking OH⁻ is at the front).

Table 1. Comparison of hydrolysis data, kinetic profile, pH_{max} and $\text{p}K_{\text{a}}$ values of different patellamide analogues.^[28]

| catalyst | pH_{max} | $v_{0,\text{max}}$ [M s^{-1}] | $\text{p}K_{\text{a}}(\text{I})$ | $\text{p}K_{\text{a}}(\text{II})$ | k_{cat} [s^{-1}] $\times 10^{-3}$ | K_{M} [mM] | $k_{\text{cat}}/K_{\text{M}}$ [$\text{M}^{-1} \text{s}^{-1}$] |
|---|--------------------------|---|----------------------------------|-----------------------------------|--|------------------------|--|
| $[\text{Cu}^{\text{II}}_2(\text{PANN}_{\text{SS}})(\text{OH})]^+$ | 6.69 | 1.4×10^{-8} | 6.3 | 7.0 | 0.4 | 5.5 | 0.07 |
| $[\text{Cu}^{\text{II}}_2(\text{PANN}_{\text{RS}})(\text{OH})]^+$ | 7.21 | 1.6×10^{-7} | 6.9 | 7.3 | 4.0 | 26.4 | 0.15 |
| $[\text{Cu}^{\text{II}}_2(\text{PAOO}_{\text{RS}})(\text{OH})]^+$ | 7.73 | 3.6×10^{-8} | 7.0 | 8.5 | 6.6 | 14.7 | 0.45 |
| $[\text{Cu}^{\text{II}}_2(\text{PASO}_{\text{RS}})(\text{OH})]^+$ | 7.57 | 3.0×10^{-8} | 7.4 | 7.7 | 2.3 | 4.2 | 0.53 |

The dependence of the energy barrier for the attack of the nucleophile at the substrate from the heterocycle in the phosphatase reaction discussed here can be traced back to a significantly larger flexibility of the $\text{Cu}^{\text{II}}\text{-N}_{\text{heterocycle}}$ bonds with the thiazole-oxazoline heterocycle combination, compared to the all-imidazole macrocycles. In dicopper(II) complexes of natural and artificial patellamides, the $\text{Cu}^{\text{II}}\text{-N}_{\text{im}}$ bonds generally are shorter than those involving the thiazole/oxazoline pair,^[18,39] and this also emerges from the DFT optimized structures (see Supporting Information, Table S1). More importantly, upon coordination of the phosphoester substrate to one of the Cu^{II} centers and attack of the OH^- nucleophile at the other Cu^{II} center, the structural rearrangements require a flexibility of the Cu^{II} ligand bonding, and the computed changes at the catalyst structures with the natural heterocycles are significantly larger than with imidazole donors (see Table S1). We hypothesize that this flexibility is the reason for the higher efficiency with the thiazole/oxazoline-based catalysts. For the much less sterically demanding carboanhydrase substrate ($\text{CO}_2/\text{CO}_3^{2-}$) flexibility is less important. This interpretation is supported by the experimental observation that phosphoester hydrolysis with sterically more demanding substrates such as the fluorescent probe DiFMUP is significantly less efficient (see below). Steric interactions along the catalytic cycle were also analyzed with noncovalent interaction plots (NCI), based on a reduced gradient analysis that has been developed to classify and visualize noncovalent interactions (for details, see Supporting Information, Figures S4–S9).^[40,41] The NCI analysis reveals important interactions between the phosphoester substrate and the macrocycle side chains (H-bonding and van der Waals interactions).

Phosphodiesterase activity

The phosphatase activity was determined with two methods, that is, an established kinetic phosphodiesterase assay using bis-2,4-dinitrophenylphosphate (BDNPP) as substrate for the time-dependent spectrophotometric determination of the concentration of 2,4-dinitrophenol,^[42–45] and a fluorometric phosphomonoester assay using 6,8-difluoro-4-methylumbelliferryl phosphate (DiFMUP) as the phosphoester substrate.^[46,47] The fluorometric assay is well-established for enzymatic phosphoester hydrolysis and was used in comparison with the established spectrophotometric method to evaluate its suitability for the patellamide-based model systems and its accuracy, specifically in an attempt to evaluate whether it can be used to accurately relate and compare *in vivo* with *ex vivo*

measurements, since *in vivo* spectrophotometric measurements in heterogenous samples such as extracts from life ascidians does not seem to be easily feasible.

Spectrophotometric kinetic data from phosphoester hydrolysis with PANN_{SS} , PANN_{RS} , PAOO_{RS} and PASO_{RS} based Cu^{II} catalysts were available from published studies,^[27,28] that is, systems that allow to compare pure imidazole and oxazole donor systems with the naturally occurring thiazole/oxazoline pair to analyze the effect of the heterocycles, and systems with all *S* as well as *R,S,R,S* configurations at the macrocycle side chain, and these appear in Table 1 (see Scheme 1 for the macrocycle structures; see Supporting Information for preliminary data with the natural ligand Asc, prepared with the methods described above).

As noted above, there is no significant dependence of the optimum pH value from the heterocyclic donor groups, that is, the two $\text{p}K_{\text{a}}$ values are largely independent from the macrocyclic donor groups (entries 1,2 vs. 3,4), and this supports the notion that for the phosphatase reactivity the choice of heterocycle primarily enforces the shape, size and flexibility of the catalytic center but does not have a noticeable electronic effect. There is a significant effect of the stereochemistry of the macrocycle side chains on the reactivity, specifically seen with $k_{\text{cat}}/K_{\text{M}}$ (entries 1 vs. 2), and the choice of heterocyclic donor also has an influence on the phosphatase activity (entries 2 vs. 3 vs. 4), see Figure 3. Importantly, the visualization of the kinetic data supports the observation based on the DFT-computed energy barrier that the influence of the side chain configuration is less pronounced than the influence of the heterocyclic

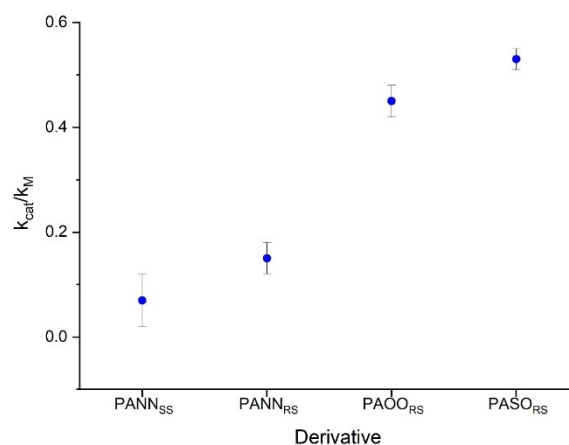


Figure 3. Comparison of the values of $k_{\text{cat}}/K_{\text{M}}$ for the BDNPP hydrolysis with different dicopper(II)-patellamide derivatives (data from Table 1).

donors, where the thiazole (and to some extent also the oxazoline) heterocycles lead to a larger and more flexible cavity (see above and Supporting Information).

The fluorometric assay with DiFMUP leads to very slow phosphoester hydrolysis with most dicopper(II)-patellamide catalysts studied here, that is, it is several orders of magnitude slower than with BDNPP (see Supporting Information). Therefore DiFMUP is not a valuable substrate for the *in vivo* evaluation of phosphatase activity by dicopper(II) patellamide complexes. Interestingly, the only catalyst with a significant reactivity towards DiFMUP is that based on PANN_{SS}, the least reactive with BDNPP. As discussed above, we assume that due to the steric demand of DiFMUP it does not fit into the cavity of the catalytic site of the dicopper(II)-patellamide catalysts, and with PANN_{SS} one side of the dicopper(II) center is open (opposite to the usual catalytic site, see Supporting Information, Figure S2). Note however that autoinhibition of the catalytic reaction by free phosphate might also play an important role in this context.^[48,49]

The entire set of computational and experimental kinetic and mechanistic data are fully consistent and allow to largely understand the reaction mechanism and reactivity trends as a function of the donor groups bound to the two copper(II) centers (imidazole vs. thiazole/oxazoline), the stereochemistry of the macrocycle side chains (*S,R,S,R* vs. *S,S,S,S*) and the substrate (BDNPP vs. DiFMUP vs. CO₂). We note however that one needs to be cautious with a unique and conclusive assessment, specifically also because the patellamide-type macrocycles have an appreciable flexibility, leading to many different possible conformations of the metal-free macrocycles and the corresponding dicopper(II) complexes. For example, in two specific conformations of the carboxylato-bridged dicopper(II) complexes, related to their carbonic anhydrase reactivity, where one was observed for the all-imidazole ligand (PANN_{SS}) and the other for the natural ascidiacyclamide, the former had a Cu^{II}–Cu^{II} distance of 5.1 Å, in the latter the Cu^{II} centers were separated by 3.6 Å. Moreover, distances obtained by EPR spectra simulation as well as from DFT optimization clearly depend on the model used (spin Hamiltonian, functional, basis set), and variations of ±0.5 Å are not unusual.^[2] All computational work done here was based on the most stable conformation of the corresponding resting state of the dicopper(II) complex, and this does not allow for large conformational changes in course of the reaction, i.e., the discussions are based on one out many possible pathways. Our assumption is that this essential restriction does not significantly influence the general interpretation given here.

Conclusion

The preparative method for patellamide derivatives described here builds on previous synthetic approaches and allows to efficiently obtain a large variety of artificial patellamide derivatives, including the naturally occurring ascidiacyclamide, straight-forwardly and in appreciable yields. The phosphoester hydrolysis activity of a range of derivatives was tested with the

usual spectrophotometric assay with BDNPP as the substrate. A fluorescence assay using DiFMUP as substrate showed that sterically demanding substrates are problematic, specifically with macrocycle derivatives that have catalytic sites with relatively small cavities and/or little flexibility. The experimentally observed reactivities are supported by DFT calculations. These indicate that the catalytic efficiencies depend on the cavity size at the catalytic center, which is enforced by the type of the macrocycle side chains and specifically by their configuration, and it is shown that the naturally occurring *R,S,R,S* configurations are generally leading to more efficient catalysts. More importantly, the naturally occurring heterocycle combination with alternating thiazole and oxazoline donors leads to the most efficient phosphatase catalysts. DFT allows to trace this to larger and more flexible cavities at the catalytic sites. Interestingly, experiments as well as DFT-based model studies show that the carbonic anhydrase activity of dicopper(II)-patellamide derivatives only depends on the stereochemistry of the macrocycle side chains, that is, it is basically independent of the heterocyclic donor groups. This is assumed to be due to the small size of the substrate in carbonic anhydrase, and it therefore supports the interpretation that the heterocyclic donors are primarily responsible for the size and flexibility of the cavity at the catalytic site.

Experimental Section

General Procedures: Chemicals used were purchased from Merck (Sigma Aldrich Chemie GmbH), Tokyo Chemical Industry Co. Ltd., Fisher Scientific GmbH, abcr GmbH, Chemos GmbH&Co.KG, Fluorochem Ltd. and Carbosynth Biosynth. Dry solvents were purchased from Arcos Organics and used as delivered. Analytical grade solvents were used without further purification and all reactions were carried out under an argon atmosphere in flame-dried glassware if not mentioned otherwise.

NMR spectra were recorded on a Bruker Avance I 200 or a Bruker Avance III 600. NMR chemical shifts are referenced on the solvents and two-dimensional correlation spectra were used to assign the signals. ESI mass spectra were recorded on a Bruker micrOTOF II: ESI Mass Spectrometer. High resolution mass spectra (HR-ESI MS) were recorded on a Finnigan MAT 8230 or JEOL JMS-700 spectrometers by Dr. Jürgen Gross and co-workers at the mass spectrometry facility of the Organic Chemistry Department of Heidelberg University.

All Flash chromatography purifications were performed using an Interchim puriFlash XS 520 with self-filled columns of appropriate size, using silica gel (30–70 nm or 70–200 nm particle size).

If not stated otherwise, the workup procedure consisted of diluting the reaction mixture with EtOAc, followed by washing the organic phase with H₂O, NaHCO₃ (aq, sat.), H₂O and brine. After drying over MgSO₄, the solvent was removed *in vacuo*.

The phosphatase-like activity was determined by spectrophotometric measurement of the hydrolysis of BDNPP. The hydrolysis product 2,4-dinitrophenolate was detected by monitoring the increase of the absorbance at 400 nm ($\epsilon = 12,100 \text{ M}^{-1} \text{ cm}^{-1}$, 25 °C). UV-vis data were recorded on a Jasco V-570 spectrophotometer equipped with a Jasco ETC-505T cryostat (set to 25 °C) and in 45:50:5 MeCN:buffer:MeOH solutions.^[28] For the newly synthesized ascidiacyclamide, the optimum pH range for phosphatase activity was determined

(see Supporting Information). The pH dependence of the catalysis rates was measured in steps of 0.25–1 pH units from pH = 4 to pH = 11 using time-course measurements at the fixed wavelength of $\lambda_{\text{max}} = 400$ nm. The stock solution concentrations of the copper(II) complexes of the cyclic pseudo-peptides was 0.8 mM (dry MeOH). The final concentrations of the dicopper(II) complexes of the ligands in the cuvette were 40 μM . For the determination of pH-dependent reaction velocities a substrate concentration of 2.5 mM (MeCN) was chosen (while this is below the optimum substrate concentration, this concentration was necessary to ensure the reproduction of previously reported solvent compositions).

Gaussian 09^[50] with B3LYP-D3 (LACVP basis set) was used for geometry optimizations and def2-TZVP for single point calculations.^[51–59] The solvation energies were computed by using the continuous polarizable continuum (CPCM) solvation model, where methanol has been used as the solvent. All reported energies are B3LYP-D3 solvent-phase energies incorporating free energy corrections at 298.15 K, unless otherwise mentioned. A Non Covalent Interactions plot (NCI Plot)^[60,61] has been used to distinguish the various non covalent interactions present in the complex.

Synthetic Methods

General Procedures (GP)

General Procedure A (Coupling): For all coupling reactions, the component with the free acid functionality (1 equiv.) was dissolved in DMF or DCM (depending on solubility), 10 mL per g of reactant. HOBt·H₂O (1.1 equiv.) and HBTU (1.1 equiv.) were added and the solution was stirred for 10 minutes. Then the second component were subsequently added (1.1 equiv. for free amines or 2.0 equiv. for allyl alcohol) as well as DIEA (2.1 equiv.). The reaction mixture was stirred over night at room temperature under an inert atmosphere. After regular workup the resulting crude product was purified by flash chromatography (EtOAc/Petrol Ether, increasing gradient 15%–>33%) to afford the clean product.

General Procedure B (Fmoc deprotection): To deprotect the Fmoc-protected peptide, the compound is dissolved in a 20% piperidine-DMF solution and rests for 30 minutes at room temperature with occasional swirling. After the solvent is removed the resulting residue was purified using a short flash chromatography column and a gradient of 15% EtOAc/PE–>33% EtOAc/PE–>10% MeOH/DCM. After removing the solvent of the MeOH/DCM fraction, the product is obtained as an orange oil.

General Procedure C (allyl deprotection): To a solution of the allyl ester (1.0 equiv.) in DCM (5 mL/mM) Pd(PPh₃)₂Cl₂ (0.025 eq) and PhSiH₃ (2 equiv.) were added resulting in a quickly darkening solution which is stirred for 6 h. After removing the solvent the resulting residue was purified using a short flash chromatography column and a gradient of 15% EtOAc/PE–>33% EtOAc/PE–>10% MeOH/DCM. After removing the solvent of the MeOH/DCM fraction, the product is obtained as a brown foam.

General Procedure D (heterocyclization): Triphenylphosphine oxide (3 equiv.) was dissolved in dry DCM (10 mL/mM) and the solution was cooled down to 0 °C followed by slow addition of trifluoromethane sulfonic anhydride (1.5 equiv.). After 10 minutes, the solution was cooled down to and kept at –20 °C using a EtOH/dry ice bath. Then, a solution of the dipeptide (1 equiv. – with the polar amino acid sidechain protected by Trt or unprotected) is slowly added. The reaction progress was monitored by TLC and usually was completed after 2–3 h. If the educt used was trityl protected, the reaction progress can also be evaluated by an increasingly

intense dark red color of the reaction mixture. After regular workup, the resulting product was purified by flash chromatography (gradient 15% EtOAc/PE–>33% EtOAc/PE–>66% EtOAc/PE).

Starting Material Fmoc-*allo*-threonin: The unprotected amino acid H₂N-*a*-Thr-OH (4.0 g, 33.6 mM) is dissolved in 75 mL of a 9% Na₂CO₃ and the solution is cooled to 0 °C using an ice bath. Fmoc-OSu (10.2 g, 30.2 mM) is dissolved in DMF (60 mL) and added dropwise to the amino acid solution. The mixture was stirred at room temperature for 2 h and diluted with ice-cold water. The aqueous solution is washed with Et₂O (60 mL), EtOAc (3×80 mL) and subsequently acidified to pH 2 at 0 °C using conc. HCl and extracted with 5×100 mL EtOAc. The combined organic layers are washed (using brine, 1 M HCl, water and brine), separated, dried with Na₂SO₄ and concentrated in vacuo to provide Fmoc-*a*Thr-OH (7.4 g, 21.7 mM, 65%) as a white solid, which was used without further purification. ¹H NMR (200 MHz, chloroform-*d*) $\delta = 7.80$ (d, *J* = 7.2, 2H), 7.63 (d, *J* = 7.2, 2H), 7.46 (d, *J* = 7.3, 2H), 7.37 (d, *J* = 7.1, 2H), 4.47 (s, 2H), 4.15 (q, *J* = 7.2, 2H), 3.76 (q, *J* = 7.0, 3H), 2.15 (s, 1H), 1.28 (d, *J* = 7.1, 3H); ESI-MS: 364.13 (M + Na⁺).

Dipeptides (Val-Cys, Ile-Ser, Ile-*a*Thr): For the synthesis of the dipeptides required for the synthesis of the heterocyclic building blocks, the polar amino acid (Cys/Ser/*a*Thr) is first allyl protected using allyl alcohol as described in GP–A (Coupling). The purified protected peptide is Fmoc-Deprotected by dissolving the peptide in MeCN (10 mL per 3 mM), adding diethylamine (10 mL per 3 mM) and stirring at room temperature until TLC shows complete deprotection (about 30 minute to ensure complete deprotection). The solution is concentrated *in vacuo* and azeotroped to dryness using MeCN, leading to a yellow-white residue which is coupled to the respective neutral amino acid following GP–A. After purification and upon concentration *in vacuo*, the dipeptides are obtained as white foams with yields between 60% and 80%, respective to the starting material and verified using ESI-MS and NMR. Fmoc-Val-Cys(STrt)-OAllyl ESI-MS: 747.17 (M + Na⁺), Fmoc-Ile-*a*Thr(OTrt)-OAllyl: ESI-MS: 759.34 (M + Na⁺), Fmoc-Ile-*a*Thr-OAllyl: ESI-MS: 517.23 (M + Na⁺), Fmoc-Ile-Ser(OTrt)-OAllyl: ESI-MS: 745.33 (M + Na⁺).

Heterocyclic Building Blocks: The heterocyclization is performed following GP-D, and is completed regardless of whether the amino acid heteroatom (S/O) was protected with Trt or unprotected. After purification the heterocyclic building blocks are obtained as oils with yields between 70% and 80% and characterized by NMR, ESI and EA.

Fmoc-Val-Thia-Oallyl: ¹H NMR (200 MHz, Chloroform-*d*) $\delta = 8.14$ (s, 1H), 7.80 (d, *J* = 7.4, 2H), 7.63 (d, *J* = 7.3, 2H), 7.52–7.29 (m, 4H), 6.23–5.93 (m, 1H), 5.67–5.26 (m, 3H), 5.06–4.82 (m, 3H), 4.49 (d, *J* = 6.9, 2H), 4.27 (d, *J* = 7.2, 1H), 2.54–2.37 (m, 2H), 1.38–1.12 (m, 1H), 0.98 (dd, *J* = 6.7, 3.4, 6H), ESI-MS: 485.21 (M + Na⁺).

HT: Fmoc-Ile-MeOxa-Oallyl: ¹H NMR (600 MHz, Chloroform-*d*) $\delta = 7.78$ –7.72 (m, 2H), 7.67–7.56 (m, 2H), 7.42–7.35 (m, 2H), 7.30 (tdd, *J* = 7.4, 5.6, 3.7, 2H), 5.91 (ddt, *J* = 16.5, 11.0, 5.9, 1H), 5.59 (d, *J* = 9.2, 1H), 5.36–5.29 (m, 1H), 5.28–5.21 (m, 1H), 4.83 (p, *J* = 6.4, 1H), 4.68–4.64 (m, 1H), 4.63 (s, 1H), 4.47–4.27 (m, 2H), 4.21 (t, *J* = 7.1, 1H), 1.58–1.45 (m, 2H), 1.45–1.09 (m, 6H), 0.97–0.85 (m, 4H), 0.82 (s, 3H). ESI-MS: 477.22 (M + H⁺), 499.23 (M + Na⁺).

HS: Fmoc-Ile-oxa-Oallyl: ¹H NMR (200 MHz, CDCl₃): δ [ppm] = 7.81 (d, 2H), 7.78 (d, 2H), 7.62 (s, 1H), 7.43 (d, 1H), 7.34 (s, 2H), 5.94 (s, 1H), 5.37 (s, 1H), 5.34 (s, 1H), 4.77 (s, 4H), 4.42 (s, 1H), 4.17 (s, 2H), 4.14 (s, 1H), 3.53 (s, 1H), 2.08 (s, 1H), 1.58 (s, 1H), 1.29 (s, 2H), 1.20 (s, 3H), 0.97 (s, 3H), ESI-MS: 485.27 (M + Na⁺).

HC: Thiazole building block Fmoc-Val-thiazole-Oallyl: The purified heterocyclic thiazoline building block derived from valine and cysteine (3.72 g, 8.0 mM, 1eq) is dissolved in dry DCM (25 mL).

MnO₂ with a maximum particle size of 10 μm is activated by heating up to at least 140 °C for 30 h, followed by an additional drying step under vacuum. This activated MnO₂ (7.1 g, 82 mM, 10.2 eq) is added to the thiazoline and the solution is stirred for at least 2 days and can be monitored via TLC or mass-spectrometric methods. After completion the MnO₂ is removed by filtration through a fritted glass filled with celite and silica gel. After concentration *in vacuo* the crude product is purified by flash chromatography (gradient 15% EE/PE–>40% EE/PE) to afford the thiazole HC (2.35 g, 5.0 mM, 64%) as a yellow oil, slowly becoming a white solid. ¹H NMR (200 MHz, chloroform-d) δ=8.14 (s, 1H), 7.80 (d, J=7.4, 2H), 7.63 (d, J=7.3, 2H), 7.52–7.29 (m, 4H), 6.23–5.93 (m, 1H), 5.59 (d, J=9.2, 1H), 5.45 (dd, J=17.2, 1.5, 1H), 5.34 (dd, J=10.3, 1.4, 1H), 4.89 (dt, J=5.8, 1.4, 2H), 4.49 (m, 2H), 4.27 (t, J=7.2, 1H), 2.54–2.37 (m, 1H), 1.38–1.12 (m, 1H), 0.98 (dd, J=6.7, 3.4, 6H). ESI-MS: 463.16 (M+H⁺).

Tetrapeptides: The heterocyclic building blocks are deprotected on one side (one N-terminally by GP-B, one O-terminally by GP-C) and after the described purification coupled to each other following general procedure A (it is worth mentioning, that better easier purification and better yields were achieved when deprotecting the thiazole building block HC at the O-terminus to obtain the free acid and the respective oxazoline at the N-terminus). This yields the dimeric compounds as white foams in yields between 55% and 75%.

Fmoc-Val-Thia-Ile-MeOxa-Oallyl (Ascidiacyclamide Dimer). ESI-MS: 681.26 (M+Na⁺)

Fmoc-Val-Thia-Ile-Oxa-Oallyl (Asc-OM Dimer) ESI-MS: 667.25 (M+Na⁺)

Octapeptides: The di-heterocyclic dimers were deprotected on both sides, first the allyl group was removed following GP-C, then the Fmoc-group was removed following GP-B. The dimer is dissolved in dry acetonitrile (10 mL per 100 mg educt), subsequently FDPP (2 equiv.) and EDIPA (E equiv.) are added, and the solution is left stirring at room temperature for at least 3 days or until TLC shows completion of the reaction. The solvent is evaporated, and the residue dissolved in EtOAc, washed with water and brine, dried over MgSO₄ and concentrated *in vacuo*. The crude product is purified by flash chromatography (gradient 20% EE/PE–>50% EE/PE, followed by DCM/EtOAc/MeOH 70/25/5) to yield the desired cyclodimerized octapeptide as an amorphous white solid with yields of 10–40%.

Ascidiacyclamide (Cyclotetramer): ¹H NMR (600 MHz, Chloroform-d) δ 8.14 (s, 2H, N_{Thia}), 7.71 (dd, J=11.4, 6.5 Hz, 2H), 7.64–7.50 (m, 1H), 5.28–5.12 (m, 1H), 5.11 (s, 1H), 4.54 (d, J=6.0 Hz, 1H), 4.47 (ttt, J=20.4, 14.1, 6.1 Hz, 1H), 4.26 (dt, J=17.5, 6.6 Hz, 1H), 3.51–3.37 (m, 2H), 2.99–2.79 (m, 2H), 2.64–2.44 (m, 2H), 1.37–1.04 (m, 12H), 0.97–0.70 (m, 24H). ¹³C NMR (151 MHz, Chloroform-d) δ 169.77, 169.22, 168.37, 160.75, 131.50, 131.32, 131.29, 131.26, 129.61, 129.60, 129.58, 129.55, 129.53, 129.49, 129.48, 129.46, 129.12, 128.21, 128.18, 128.15, 128.11, 128.10, 128.08, 128.07, 128.06, 128.03, 127.93, 127.26, 127.07, 126.95, 126.93, 126.91, 126.86, 126.83, 120.35, 119.98, 119.00, 118.95, 118.83, 118.74, 118.47, 118.37, 79.90, 70.61, 69.39, 51.42, 48.51, 31.05, 30.23, 29.98, 20.31, 19.86, 18.63. ESI-MS: (calculated: 757.352 (M+H); measured: 757.357 (M+H))

Asc-OM (Cyclotetramer). ESI-MS 747.44 (M+H⁺+H₂O).

Supporting Information: The Supporting Information includes all experimental details of the phosphatase kinetics with the dicopper(II) complex of Asc with BDNPP and of the complexes with PANN_{SS}, PANN_{RS} and Asc with DiFMUP, a structural analysis of the systems with PANN_{SS} and Asc, involving the resting state, the two

intermediates with coordinated substrate and the corresponding transition states as well as details to the computational study.

Acknowledgements

Financial support by Heidelberg University and the Max Planck School Matter to Life is gratefully acknowledged. This study was conducted within the Max Planck School Matter to Life, supported by the German Federal Ministry of Education and Research (BMBF) in collaboration with the Max Planck Society. We are grateful for computational resources provided by the bwForCluster JUSTUS, funded by the Ministry of Science, Research and Arts and the Universities of the State of Baden-Württemberg, Germany, within the framework program bwHPC-C5. Open Access funding enabled and organized by Projekt DEAL.

Conflict of Interest

The authors declare no conflict of interest.

Data Availability Statement

The data that support the findings of this study are available in the supplementary material of this article.

Keywords: patellamide · cyclic peptide · dinuclear copper(II)complex · phosphatase · DFT calculation

- [1] C. M. Ireland, A. R. Durso, R. A. Newman, M. P. Hacker, *J. Org. Chem.* **1982**, *47*, 1807–1811.
- [2] P. Comba, N. Dovalil, L. R. Gahan, G. Haberhauer, G. R. Hanson, C. J. Noble, B. Seibold, P. Vadivelu, *Chem. Eur. J.* **2012**, *18*, 2578–2590.
- [3] P. Comba, N. Dovalil, L. R. Gahan, G. R. Hanson, M. Westphal, *Dalton Trans.* **2014**, *43*, 1935–1956.
- [4] P. Comba, A. Eisenschmidt, L. R. Gahan, D.-P. Hertzen, G. Nette, G. Schenk, M. Seefeld, *Chem. Eur. J.* **2017**, *23* (Special Issue 150 Years German Chemical Society), 12264–12274.
- [5] P. Comba, A. Eisenschmidt, in *Future Directions in Metalloprotein and Metalloenzyme Research*, *Biological Magnetic Resonance*, Vol 3 (Ed.: G. B. Hanson, L. Berliner), Springer, Heidelberg, **2017**, 13–32.
- [6] P. Baur, M. Kühl, P. Comba, L. Behrendt, *Mar. Drugs* **2022**, *20*, 119.
- [7] M. Jaspers, L. A. Morris, *RSC Special Publ.* **2000**, 140–166.
- [8] E. W. Schmidt, J. T. Nelson, D. A. Rasko, S. Sudek, J. A. Eisen, M. G. Haygood, J. Ravel, *Proc. Nat. Acad. Sci.* **2005**, *102*, 7315–7320.
- [9] M. Kühl, L. Behrendt, E. Trampe, K. Qvortrup, U. Schreiber, S. M. Borisov, I. Klimant, A. W. Larkum, *Front. Microbiol.* **2012**, *3*, 402.
- [10] P. Comba, L. R. Gahan, G. R. Hanson, M. Maeder, M. Westphal, *Dalton Trans.* **2014**, *43*, 3144–3152.
- [11] P. Comba, N. Dovalil, G. Hanson, J. Harmer, C. J. Noble, M. J. Riley, B. Seibold, *Inorg. Chem.* **2014**, *53*, 12323–12336.
- [12] P. Wipf, C. P. Miller, *Tetrahedron Lett.* **1992**, *7*, 907–910.
- [13] Y. Hamada, M. Shibata, T. Shioiri, *Tetrahedron Lett.* **1985**, *26*, 5155–5158.
- [14] L. R. Gahan, R. M. Cusack, *Polyhedron* **2018**, *153*, 1–23.
- [15] S. Xie, A. I. Savchenko, M. Kerscher, R. L. Grange, E. H. Krenske, J. R. Harmer, M. J. Bauer, N. Broit, D. J. Watters, J. M. Boyle, P. V. Bernhardt, P. G. Parson, P. Comba, L. R. Gahan, C. M. Williams, *Eur. J. Org. Chem.* **2018**, 1465–1476.
- [16] M. S. VanNieuwenhze, P. García-Reynaga, *Org. Lett.* **2008**, *10*, 4621–4623.
- [17] G. Haberhauer, F. Rominger, *Eur. J. Org. Chem.* **2003**, 3209–3218.

- [18] P. Comba, N. Dovalil, G. R. Hanson, G. Linti, *Inorg. Chem.* **2011**, *50*, 5165–5174.
- [19] S. L. You, J. W. Kelly, *J. Org. Chem.* **2003**, *68*, 9506–9509.
- [20] S.-L. You, H. Razavi, J. W. Kelly, *Angew. Chem. Int. Ed.* **2003**, *42*, 83–85; *Angew. Chem.* **2003**, *115*, 87–89.
- [21] J. B. Hendrickson, S. M. Schwartzman, *Tetrahedron Lett.* **1975**, 273–276.
- [22] J. B. Hendrickson, M. S. Hussoin, *Synlett* **1990**, 423–424.
- [23] J. B. Hendrickson, M. A. Walker, A. Varvak, M. S. Hussoin, *Synlett* **1996**, 661–662.
- [24] F. Yokokawa, Y. Hamada, T. Shioiri, *Synlett* **1992**, 153–155.
- [25] M. North, G. Pattenden, *Tetrahedron* **1990**, *46*, 8267–8290.
- [26] C. D. J. Boden, G. Pattenden, T. Ye, *Synlett* **1995**, 417–419.
- [27] P. Comba, L. R. Gahan, G. R. Hanson, M. Westphal, *Chem. Commun.* **2012**, *48*, 9364–9366.
- [28] P. Comba, A. Eisenschmidt, L. Gahan, G. Hanson, N. Mehrkens, M. Westphal, *Dalton Trans.* **2016**, *45*, 18931–18945.
- [29] P. Comba, A. Eisenschmidt, N. Kipper, J. Schiessl, *J. Inorg. Biochem.* **2016**, *159*, 70–75.
- [30] P. M. Dewick, *Essentials of Organic Chemistry: For Students of Pharmacy, Medicinal Chemistry and Biological Chemistry*, John Wiley & Sons Inc, **2006**.
- [31] Calculated using Advanced Chemistry Development (ACD/Labs) Software V11.02 © 1994–2021 ACD/Labs via CoAS Scifinder.
- [32] Note that methyl-substituted heterocycles have slightly different pK_a values. Note also that the imidazole heterocycles only occur in synthetic model compounds.^[3]
- [33] A. L. van den Brenk, K. A. Byriel, D. P. Fairlie, L. R. Gahan, G. R. Hanson, C. J. Hawkins, A. Jones, C. H. L. Kennard, B. Moubaraki, K. S. Murray, *Inorg. Chem.* **1994**, *33*, 3549–3557.
- [34] P. V. Bernhardt, P. Comba, T. W. Hambley, S. S. Massoud, S. Stebler, *Inorg. Chem.* **1992**, *31*, 2644–2651.
- [35] P. Comba, M. Kerscher, Y. D. Lampeka, L. Lötzbeier, H. Pritzkow, L. V. Tsybal, *Inorg. Chem.* **2003**, *42*, 3387–3389.
- [36] P. Comba, Y. D. Lampeka, A. Prikhod'ko, G. Rajaraman, *Inorg. Chem.* **2006**, *45*, 3632–3638.
- [37] P. Comba, R. Cusack, D. P. Fairlie, L. R. Gahan, G. R. Hanson, U. Kazmaier, A. Ramlow, *Inorg. Chem.* **1998**, *37*, 6721–6727.
- [38] P. Comba, A. Eisenschmidt, G. Velmurugan, Unpublished Results.
- [39] G. Abbenante, D. P. Fairlie, L. R. Gahan, G. R. Hanson, G. K. Pierens, A. L. van den Brenk, *J. Am. Chem. Soc.* **1996**, *118*, 10384–10388.
- [40] F. Biegler-König, J. Schönbohm, D. Bayles, *J. Comput. Chem.* **2001**, *22*, 545–559.
- [41] S. Kozuch, J. M. Martin, *J. Chem. Theory Comput.* **2013**, *9*, 1918.
- [42] N. V. Kaminskaya, B. Spingler, S. J. Lippard, *J. Am. Chem. Soc.* **2000**, *122*, 6411–6422.
- [43] L. J. Daumann, L. R. Gahan, P. Comba, G. Schenk, *Inorg. Chem.* **2012**, *51*, 7669–7681.
- [44] L. J. Daumann, P. Comba, J. A. Larrabee, G. Schenk, R. Stranger, G. Cavigliasso, P. V. Bernhardt, L. R. Gahan, *Inorg. Chem.* **2013**, *52*, 2029–2043.
- [45] S. C. Batista, A. Neves, A. J. Bortoluzzi, I. Vencato, R. A. Peralta, B. Szpoganicz, V. V. E. Aires, H. Terenzi, P. C. Severino, *Inorg. Chem. Commun.* **2003**, *6*, 1161–1165.
- [46] S. Welte, K. H. Baringhaus, W. Schmider, G. Müller, S. Petry, N. Tennagels, *Anal. Biochem.* **2005**, *338*, 32–38.
- [47] K. Gee, W.-C. Sun, M. K. Bhalgat, R. H. Upson, D. H. Klaubert, K. A. Latham, R. P. Haugland, *Anal. Biochem.* **1999**, *273*, 41–48.
- [48] Y. In, M. Doi, M. Inoue, T. Ishida, Y. Hamada, T. Shioiri, *Chem. Pharm. Bull.* **1993**, *41*, 1686–1690.
- [49] S. P. Coburn, J. D. Mahuren, M. Jain, Y. Zubovic, J. Wortsman, *J. Clin. Endocrinol. Metab.* **1998**, *83*, 3951–3957.
- [50] M. J. Frisch, G. W. Trucks, H. B. Schlegel, G. E. Scuseria, M. A. Robb, J. R. Cheeseman, G. Scalmani, V. Barone, B. Mennucci, G. A. Petersson, H. Nakatsuji, M. Caricato, X. Li, H. P. Hratchian, A. F. Izmaylov, J. Bloino, G. Zheng, J. L. Sonnenberg, M. Hada, M. Ehara, K. Toyota, R. Fukuda, J. Hasegawa, M. Ishida, T. Nakajima, Y. Honda, O. Kitao, H. Nakai, T. Vreven, J. A. Montgomery Jr., J. E. Peralta, F. Ogliaro, M. Bearpark, J. J. Heyd, E. Brothers, K. N. Kudin, V. N. Staroverov, R. Kobayashi, J. Normand, K. Raghavachari, A. Rendell, J. C. Burant, S. Iyengar, J. Tomasi, M. Cossi, N. Rega, N. J. Millam, M. Klene, J. E. Knox, J. B. Cross, V. Bakken, C. Adamo, J. Jaramillo, R. Gomperts, R. E. Stratmann, O. Yazyev, A. J. Austin, R. Cammi, C. Pomelli, J. W. Ochterski, R. L. Martin, K. Morokuma, V. G. Zakrzewski, G. A. Voth, P. Salvador, J. J. Dannenberg, S. Dapprich, A. D. Daniels, O. Farkas, J. B. Foresman, J. V. Ortiz, J. Cioslowski, D. J. Fox, *Gaussian 09, Revision D.01*, Gaussian, Inc., Wallingford CT, **2013**.
- [51] P. J. Hay, W. R. Wadt, *J. Chem. Phys.* **1985**, *82*, 270–283.
- [52] W. R. Wadt, P. J. Hay, *J. Chem. Phys.* **1985**, *82*, 284–298.
- [53] P. J. Hay, W. R. Wadt, *J. Chem. Phys.* **1985**, *82*, 299–310.
- [54] R. Ditchfield, W. J. Hehre, J. A. Pople, *J. Chem. Phys.* **1971**, *54*, 724–728.
- [55] S. Grimme, J. Antony, S. Ehrlich, H. Krieg, *J. Chem. Phys.* **2010**, *132*, 154104.
- [56] A. D. Becke, *Phys. Rev. A* **1988**, *38*, 3098–3100.
- [57] J. P. Perdew, *Phys. Rev. B* **1986**, *33*, 8822–8824.
- [58] J. Zheng, X. Xu, D. G. Truhlar, *Theor. Chem. Acc.* **2011**, *128*, 295–305.
- [59] I. Shimizu, Y. Morimoto, G. Velmurugan, T. Gupta, S. Paria, T. Ohta, H. Sugimoto, N. Fujieda, T. Ogura, P. Comba, S. Itoh, *Chem. Eur. J.* **2019**, *25*, 11157–11165.
- [60] J. Contreras-García, E. R. Johnson, S. Keinan, R. Chaudret, J. P. Piquemal, D. N. Beratan, W. Yang, *J. Chem. Theory Comput.* **2011**, *7*, 625–632.
- [61] E. R. Johnson, S. Keinan, P. Mori-Sánchez, J. Contreras-García, A. J. Cohen, W. Yang, *J. Am. Chem. Soc.* **2010**, *132*, 6498–6506.

Manuscript received: January 25, 2022

Accepted manuscript online: February 18, 2022

Version of record online: March 18, 2022